The Diffraction of X-Rays by Liquid Elements

NEWELL S. GINGRICH

University of Missouri, Columbia, Missouri

I. INTRODUCTION

DISCOVERY of diffraction and interference effects associated with the passage of x-rays through matter very soon led to the recognition that studies of these effects are useful in determining the structure of matter. Work on the diffraction of x-rays by crystals was initiated in 1912 with the famous discovery made by Friedrich, Knipping, and Laue[1] and this field has been developed extensively[2] by many investigators to supply valuable information concerning the arrangements of atoms in crystals. Diffraction of x-rays by gases was first studied as early as 1911,[3] and subsequent work in this field[4] has supplied information not only on the arrangements of atoms in molecules, but also on the electron distributions within atoms. Early work on the diffraction of x-rays by liquids and non-crystalline substances dates back to 1913 when Friedrich[5] obtained x-ray diffraction patterns of Canada balsam, paraffin, and amber. In 1916, Debye and Scherrer[6] obtained diffraction patterns of several liquids, including benzene, and in 1922, Keesom and de Smedt[7] reported work of this type with liquid elements. Subsequent experimental investigations and theories in this field have made possible the determination of atomic distributions in liquids, giving results which are perhaps the most quantitative means at our disposal of describing the structure of a liquid.

Although x-ray diffraction patterns of many liquids have been studied, the present discussion is limited almost exclusively to liquid elements. The early work of Keesom and de Smedt[7] on nitrogen, oxygen, and argon supplied valuable qualitative information concerning the structure of liquid elements, but the theoretical advances made by Zernike and Prins[8] and by Debye and Menke[9] supplied a strong impetus to further study in this field because they offered a quantitative approach to the interpretation of experimental results. Within the decade following these theoretical advances, experimental studies were carried out on helium, lithium, nitrogen, oxygen, sodium, aluminum, phosphorus, sulphur, chlorine, argon, potassium, zinc, gallium, selenium, rubidium, cadmium, indium, tin, cesium, mercury, thallium, lead, and bismuth. In the cases of many of these elements, the available quantitative interpretation was applied, and in some cases, the effect of temperature on the liquid structure was investigated. For the two elements, argon and nitrogen, the effect of pressure was also investigated, including the case where the element was a permanent gas at high pressure.

Studies of x-ray diffraction by liquid elements have certain advantages over those with polyatomic liquids. In the first place, the theory by means of which the atomic distribution is obtained from the diffraction pattern, is more simply and accurately applied to an assemblage of atoms of one kind than to a polyatomic liquid, since fewer assumptions are required. In the second place, theoretical considerations concerning liquid structures and the nature of interatomic forces are more likely to deal with the simplest liquids than with the more complicated ones. This estimate has already been borne out, notably in the cases of argon, sodium, potassium, and mercury for which theoretical work has supplied interesting and valuable comparisons with, or deductions from, the experimentally determined atomic distribution functions. Finally, it is important to have as full and complete information as possible concerning the properties of all the elements.

II. THEORY

Although many investigators[10] have contributed to discussions of the theory of x-ray diffraction by liquids, the most fruitful approach to the present problem is that which had its origin with the early work of Debye[11] in which it was shown that one has always to consider two atoms whose scattered rays interfere with one another as a result of which an interference pattern is produced which is defined essentially by the relative

separations of the two atoms. If the relative frequency with which various relative separations occurred were known completely, then the intensity patterns could be predicted. Zernike and Prins[8] proved in a one-dimensional model that certain distances receive special weight in the formation of interferences, and it is clear that this conclusion can be carried over, at least qualitatively, to three-dimensional liquids, since the impossibility of interpenetration of atoms and the existence of interatomic binding imply that certain arrangements of any given atom with respect to its neighbors are more probable than others. These investigators introduced the idea of a distribution function which, if known, would facilitate prediction of the x-ray pattern to be expected for any given substance. But even in the simplest case of atoms as hard spheres, it has not been possible to calculate unambiguously and exactly the distribution of atoms about any given atom, and hence this method can so far supply only qualitative results. If, however, the x-ray intensity curve is known precisely, then the reverse of the above procedure is available, and the distribution function can be determined from the experimental intensity curves. This was suggested by Zernike and Prins as a possibility, but it remained for Debye and Menke[9] to complete the analysis and to apply it for the first time to liquid mercury. An alternative presentation of this theory has been given by Warren and Gingrich[12] and by Warren,[13] and this is the one followed here.

Consider an incident x-ray beam of amplitude E_0 propagated in a direction defined by the unit vector S_0, polarized with its electric field normal to the plane of Fig. 1, and directed upon an atom at O. For a single electron at O, the amplitude of the radiation scattered to a point P at a large distance R from O and in a direction defined by the unit vector S is given by electromagnetic theory[14] as

$$E_p = E_0(e^2/mc^2R). \qquad (1)$$

If Z electrons were concentrated at O, then the amplitude of the scattered radiation at P would be Z times as great as for one electron. But for an atom of atomic number Z at O, the size of the atom is comparable to the wave-length of
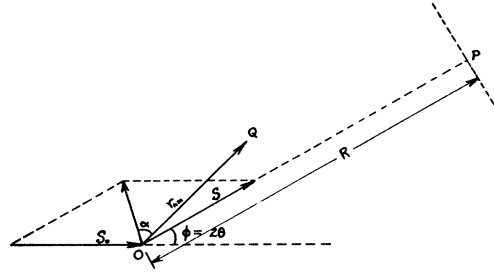
FIG. 1. Unit vector S_0 defines the direction of radiation incident upon an atom at O; unit vector S defines the direction of radiation scattered at angle ϕ; vector r_{nm} represents the interatomic displacement between atoms at O and Q.

x-rays, and hence there will be interference effects between the rays scattered by different electrons in the same atom. The resultant amplitude at P is then given by

$$E_p = E_0 f(e^2/mc^2R), \qquad (2)$$

where the factor f, called the atomic structure factor, is determined by the distribution of electrons in the atom, and is equal to, or less than Z. The phase of the radiation scattered from atom n at Q as compared to that from the origin atom is $2\pi/\lambda(r_n \cdot S_0 - r_n \cdot S)$, and thus, if there is an incident wave of the form $E = E_0 \exp (2\pi i\nu t)$, the scattered wave from atom n is given by

$$E_p = E_0(e^2/mc^2R)f_n$$
$$\times \exp [2\pi i(\nu t - r_n \cdot (S_0 - S)/\lambda)]. \qquad (3)$$

The total amplitude at P is the sum of all the amplitudes scattered to that point and is given by

$$E_p = E_0(e^2/mc^2R)\sum_n f_n$$
$$\times \exp [\{2\pi i/\lambda\}(S - S_0) \cdot r_n] \qquad (4)$$

and the square of the amplitude of the radiation at P is obtained by multiplying (4) by its complex conjugate, giving

$$E_p{}^2 = E_0{}^2(e^4/m^2c^4R^2)$$
$$\times [\sum_n f_n \exp (\{2\pi i/\lambda\}(S - S_0) \cdot r_n)]$$
$$\times [\sum_m f_m \exp (\{2\pi i/\lambda\}(S - S_0) \cdot r_m)]. \qquad (5)$$

Removing the restriction of plane polarized radiation introduces the polarization factor derived

elsewhere[14] and we have

$$E_p{}^2 = \{(1+\cos^2 \phi)/2\}$$

$$\times E_0{}^2(e^4/m^2c^4R^2)\sum_n \sum_m f_n f_m$$

$$\times \exp\left[\{2\pi i/\lambda\}(S-S_0)\cdot(r_n-r_m)\right]. \quad (6)$$

The coefficient of the double summation is proportional to the intensity scattered by a single electron, represented by I_e, and $E_p{}^2$ is proportional to the intensity of scattered radiation I. Furthermore, $r_n-r_m=r_{nm}$, $S-S_0=2\sin\theta$, where θ is half the scattering angle, s is defined as $(4\pi\sin\theta)/\lambda$, and α is the angle between $(S-S_0)$ and r_{nm}. Then if I/I_e is designated I_{eu}, intensity in electron units, Eq. (6) may be written as

$$I_{eu} = \sum_n \sum_m f_n f_m \exp(i s r_{nm} \cos \alpha). \quad (7)$$

Now, as the vector r_{nm} takes on all positions in space, α takes on all values at random, and the effect of this random orientation may be obtained by averaging the exponential function over all solid angle. Thus

$$\int_0^{4\pi} [\exp(i s r_{nm} \cos \alpha)]d\Omega \Big/ \int_0^{4\pi} d\Omega$$

$$= \int_0^{\pi} [\exp(i s r_{rm} \cos \alpha)]2\pi \sin \alpha d\alpha/4\pi$$

$$= (\sin s r_{nm})/s r_{nm}$$

and hence we have Debye's equation

$$I_{eu} = \sum_n \sum_m f_n f_m \{(\sin s r_{mn})/s r_{mn}\}. \quad (8)$$

It is seen that the intensity depends upon the structure factors of the atoms, the angle of scattering, the wave-length of the x-rays, and upon the interatomic distances r_{nm}. In the present discussion for atoms of one kind, $f_n=f_m=f$, and $f_n f_m=f^2$.

In performing the summations, it is necessary to consider one atom and to carry out the summation over all distances to all atoms of the array, including the origin atom, and then to allow the origin atom to be every atom in the array in turn. Summations for any atom with respect to itself lead simply to unity in each case since in the limit as $r_{nm}\to 0$, $\sin s r_{nm}/s r_{nm}\to 1$. Thus, if there are N atoms in the array,

$$I_{eu} = Nf^2[1+\sum_n{}' (\sin s r_{nm})/s r_{nm}], \quad (9)$$

where this summation excludes the origin atom. If it is assumed that there is a continuous distribution of atoms, then the above summation may be replaced by an integral. If $\rho(r)$ is the density of atoms at distance r from the origin atom, then the number of atoms in a spherical shell of radius r and thickness dr is $4\pi r^2\rho(r)dr$, and this is sometimes referred to as the radial density of atoms, or the atomic distribution function.

Equation (9) is then written as

$$I_{eu} = Nf^2\left[1+\int_0^R 4\pi r^2\rho(r)\{(\sin s r)/s r\}dr\right], \quad (10)$$

where R is the radius of the liquid sample, which is very large compared to any value of r of interest here. If we take ρ_0 as the constant average density of atoms, then Eq. (10) may be rewritten

$$I_{eu} = Nf^2\left[1+\int_0^R 4\pi r^2(\rho(r)-\rho_0)\{(\sin s r)/s r\}dr\right.$$

$$\left.+\int_0^R 4\pi r^2\rho_0\{(\sin s r)/s r\}dr\right]. \quad (11)$$

The second integral may be taken as zero, under normal conditions, for physical reasons. It is seen that

$$\int_0^R 4\pi r^2\rho_0\{(\sin s r)/s r\}dr = \left[(4\pi r^3/3)\rho_0(3/(s r)^2)\right.$$

$$\left.\times(\{(\sin s r)/s r\}-\cos s r)\right]_{r=0}^{r=R}. \quad (12)$$

For $r=0$, this is zero regardless of s, and for $r=R$, a very large quantity, the integral is zero unless s is extremely small. For s corresponding to a scattering angle of the order of minutes or seconds of arc, this integral should contribute to the intensity pattern, but this portion of the intensity pattern is wholly unobservable because of the presence of the main beam. For normal sample sizes, and as long as we limit ourselves to observable intensity, this integral may then be taken as zero.

Equation (11) may be rearranged into a more useful form by writing

$$i(s) = (I_{eu}/Nf^2) - 1 \quad (13)$$

and by taking the limits as 0 to ∞ instead of 0 to R. This change of limit is necessary for later application of the Fourier integral theorem, and it is justified by the fact that $\rho(r)$ rapidly approaches ρ_0 as r reaches several atomic diameters, which is still many orders of magnitude less than R. Then

$$si(s) = \int_0^\infty 4\pi r(\rho(r) - \rho_0) \sin srdr, \qquad (14)$$

which is transformed by the Fourier integral theorem into

$$r\{\rho(r) - \rho_0\} = (1/2\pi^2)\int_0^\infty si(s) \sin rsds \qquad (15)$$

or

$$4\pi r^2\rho(r) = 4\pi r^2\rho_0 + (2r/\pi)\int_0^\infty si(s) \sin rsds. \qquad (16)$$

Equation (16) is the one which has been used extensively in the determination of the distribution function $4\pi r^2\rho(r)$ giving the number of atoms between r and $r+dr$ from any arbitrary atom within the liquid element. Two important steps remain to complete this determination; first, the evaluation of the function $i(s)$ from experiment, and second, the evaluation of the integral of Eq. (16).

III. EXPERIMENTAL

Inspection of the theoretical development shows that the following experimental conditions are called for: (1) monochromatic x-rays, (2) well-defined directions of incidence and scattering, (3) a true measure of the coherently scattered intensity from the liquid element as a function of s over a very wide range of s, (4) no distortion in the relative intensity measurements due, for example, to polarization or absorption effects, (5) the same units for I and Nf^2 of Eq. (13). These are some of the more important conditions to be considered and met as closely as possible.

A. Radiation

Radiation from an x-ray tube target is made up of continuous radiation and characteristic (or line) radiation and two methods have been used to attempt to satisfy condition (1) above, first, crystal reflection, and second, selective filtering. Generally, high intensities have been attained with the second method by using a band of wavelengths, but this does not satisfy condition (1) Crystal reflection does supply monochromatic radiation as long as the voltage on the x-ray tube is lower than that which is necessary to excite continuous radiation of one-half the wavelength of the desired characteristic radiation. Furthermore, it has been shown[15] that improper filtering can give rise to spurious diffraction peaks, and that filtering to obtain monochromatic radiation closely approximate to that obtained by crystal reflection is not as efficient as crystal reflection itself in the matter of exposure time. Although several different crystal monochromators have been tried, rocksalt appears to be the most suitable for this purpose.

The choice of characteristic radiation to be used is determined largely by considerations of available targets, absorption in the sample, and the region of s to be emphasized. Thus, for detailed investigation of scattering at small values of s, long wave-lengths such as that of Cu are useful. For emphasis on scattering at large s, a short wave-length such as that of Ag is useful, and for general purposes, Mo radiation is quite suitable.

Unpolarized radiation from the x-ray target undergoes partial polarization when scattered by the liquid sample, and also when reflected from the crystal monochromator if this is used. It is shown elsewhere[14] that the polarization factor is $(1 + \{\cos^2 2\theta\}/2)$ for scattering from the sample. If 2ψ is the total angle of scattering from the crystal, it can be proved that this factor should be $\{1 + (\cos^2 2\psi \cos^2 2\theta)/2\}$. That this is so can be seen qualitatively from the fact that only the component of the electric field (in the electromagnetic x-radiation) normal to the plane of scattering remains unaltered, while the component in the plane of scattering may suffer a diminution at each scattering. Since scattered intensity with no effect of polarization is desired, the experimental intensity is to be divided by whichever of the above two factors is appropriate under particular experimental conditions.

B. Detectors of Radiation

Photographic film has been the most commonly used agency for detection of radiation in this field of work. Cylindrical cameras are used, with the sample at the center of the cylinder, and with the film on the circumference. For accurate measurement of diffraction angles, a fairly large camera, of perhaps 9-cm radius, is desirable. It has been demonstrated[16] that (1) ordinary x-ray film responds faithfully for reasonable densities of exposure, that (2) double-emulsion type film is considerably more effective than ordinary films for Mo radiation, and that (3) the use of intensifying screens for the measurement of relative intensities introduces almost insurmountable complications. Careful microphotometering of the films is, of course, a necessary adjunct to this method.

Electrical methods of detection are available, and in this category, a Geiger-Mueller counter[17] has been used successfully for x-ray diffraction by a liquid element. Considerable preparation must be made for this method, but where temperatures and pressures of the sample must be accurately maintained, the shorter time required to obtain a complete pattern, as compared with the photographic method, may justify this preparation.

C. The Sample

Many different types of samples have been used to meet the special requirements of the various liquid elements. In the case of He, no container was used, but a free stream of the liquid constituted the sample. Unfortunately it is not practical to adopt this ideal scheme for many elements. Cylindrical glass tubes of very thin walls have been used, with diameters ranging from about 0.05 cm to 0.3 cm and with wall thicknesses ranging between 0.002 cm and 0.01 cm in various cases. For Li, a cell of triangular section in a horizontal plane was used with a maximum thickness of 1.8 cm. In this case, the size of the sample constituted an appreciable fraction of the camera radius, and hence the pattern was probably somewhat smeared out because of the poor geometrical conditions. In some instances, flat cells were used, with the incident beam making an angle of 90° or less

with the plane of the cell. With this arrangement, cell thicknesses were from 0.17 cm to 0.008 cm, with mica windows 0.0005 cm thick, or with Be windows 0.03 cm to 0.07 cm thick. In addition to the above schemes for transmission, diffraction patterns have also been obtained by reflection from liquid surfaces, as was done in the case of mercury.

1. Optimum Thickness

The transmission method has been used most frequently, and in this case there is an optimum thickness of cell, since a cell which is too thin
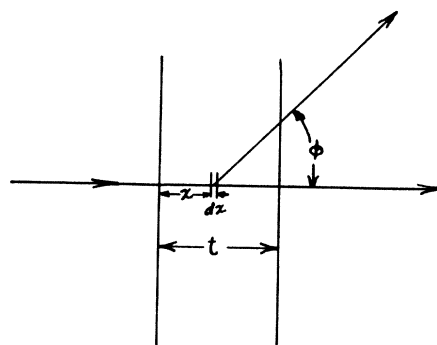
FIG. 2. Representing scattering at an angle ϕ from a layer of thickness dx at a depth x in a flat sample of thickness t. The incident beam is perpendicular to the plane of the sample.

has insufficient scattering matter, and since one of great thickness absorbs too strongly. Consider the case of a flat sample of thickness t and linear absorption coefficient μ with an incident beam of intensity I_0 directed perpendicularly upon the sample, as in Fig. 2. Then a thickness dx at depth x will contribute to the intensity scattered at angle $\phi = 2\theta$ in the amount dI_ϕ where

$$dI_\phi = [cI_0 \exp (-\mu x)dx](\exp [-\mu(t-x)/\cos \phi])$$

or

$$I_\phi = K[\exp (-\mu t) - \exp (-\mu t/\cos \phi)],$$

and

$$K = (cI_0 \cos \phi)/\mu(1 - \cos \phi).$$

Applying the condition for optimum thickness,

$$dI_\phi/dt = K[-\mu \exp (-\mu t_0)$$

$$+ (\mu/\cos \phi) \exp (-\mu t_0/\cos \phi)] = 0$$

and hence

$$t_0 = (1/\mu)[-(\cos \phi \log \cos \phi)/(1 - \cos \phi)], \quad (17)$$

which, in the limit as ϕ approaches 0, is $t_0 = 1/\mu$. Thus, for scattering at small angles, the optimum thickness is the reciprocal of the linear absorption coefficient, but for other scattering angles, it is less than $1/\mu$. Figure 3 shows the optimum thickness as a function of scattering angle ϕ. If the plane of the flat sample is not perpendicular to the incident beam, then the above relation should be modified to meet this condition. For a cylindrical sample completely bathed in incident radiation, the expression $t_0 = 1/\mu$ should be a good approximation to the optimum diameter for very small values of ϕ, but experience shows that a cylinder of diameter as much as two or three times t_0 gives more intense patterns than one of t_0. This is presumably due to the fact that one is generally interested in the diffraction pattern at points considerably removed from the incident beam, for which the above expression for optimum thickness is not valid.

2. Absorption Corrections

Inasmuch as the rays scattered at different angles suffer different amounts of absorption in the sample itself, the true relative intensity of one portion of the pattern with respect to that of another can be obtained only after correction for this differential absorption.

Consider first, the case of a flat sample of thickness t with the normal to its surface making an angle σ with the direction of the incident beam as shown in Fig. 4. If the incident beam is
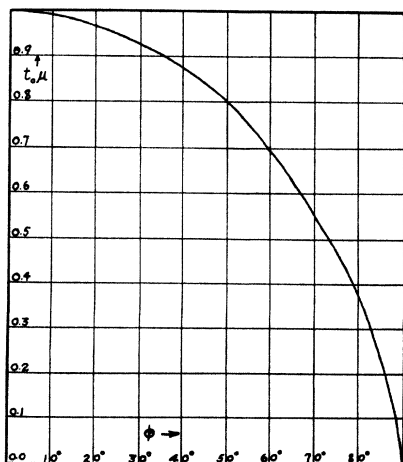
FIG. 3. Showing how optimum thickness of a flat sample varies with the scattering angle.
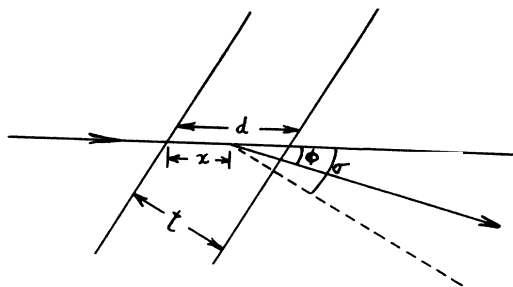
FIG. 4. Directions and angles defined for the computation of the absorption correction in a flat sample whose normal is inclined at an angle σ with the direction of incident radiation.

of original intensity I_0, the contribution to the intensity scattered at angle ϕ by a thickness dx at depth x in the sample is

$$dI_\phi = K[\exp(-\mu x)dx]$$

$$\times \{\exp[-\{\mu(d-x)\cos\sigma\}/\cos(\sigma-\phi)]\}, \quad (18)$$

where K includes I_0 and other constant factors. Then

$$I_\phi = K \exp[-\mu d \cos\sigma/\cos(\sigma-\phi)]$$

$$\int_0^d \exp\{\mu x[\cos\sigma - \cos(\sigma-\phi)]/$$
$$\cos(\sigma-\phi)\}dx, \quad (19)$$

or

$$I_\phi = K/\mu z \cos\sigma$$

$$\times \{\exp[-\mu d \cos\sigma/\cos(\sigma-\phi)]\}$$

$$\times [\exp(\mu z d \cos\sigma) - 1], \quad (20)$$

where

$$z = [\cos\sigma - \cos(\sigma-\phi)]/\cos\sigma \cos(\sigma-\phi).$$

Since relative intensity is desired, it is necessary to normalize the above expression with respect to some particular direction. We refer the intensity at any angle ϕ to that at $\phi = 0$. From Eq. (19) it is seen that for $\phi = 0$,

$$I_{\phi=0} = Kde^{-\mu d} \quad (21)$$

and, noting that $t = d \cos\sigma$, we have

$$I_\phi/I_{\phi=0} = (1/\mu tz)[1 - e^{-\mu tz}]. \quad (22)$$

This relation may be used with the sample perpendicular to the main beam, for in this case, $\sigma = 0$ and $z_\perp = (1 - \cos\phi)/\cos\phi$. When $\sigma \neq 0$, an alternative procedure is to normalize with re-

spect to the intensity at $\phi = \sigma$. Setting $\phi = \sigma$ in Eq. (20) and taking the ratio of I_ϕ to $I_{\phi=\sigma}$, we have,

$$I_\phi/I_{\phi=\sigma} = \{(\cos \sigma - 1)/\cos \sigma[\exp (-\mu t)$$

$$-\exp (\mu t \cos \sigma)]\}\{[\exp \{-\mu t/\cos (\sigma - \phi)\}]$$

$$\times [\exp (\mu z t) - 1]/z\}. \quad (23)$$

The experimental intensity is to be corrected by dividing it by Eq. (22) or Eq. (23), and this correction can be made along with the polarization correction described above. This corrected intensity is that which one would observe if there were no effect of absorption or polarization.

In the reflection method, assume that all rays strike the liquid surface at an angle α. A volume element $(A\,dx)/\sin \alpha$ at a depth x below the surface will be irradiated by primary rays which have traveled a distance $x/\sin \alpha$ in the liquid, and a secondary ray scattered at an angle 2θ with the primary beam travels through the liquid a distance $x/\sin (2\theta - \alpha)$ before reaching the surface. The intensity of rays scattered at angle 2θ is therefore

$$I_{2\theta} = K(1/\sin \alpha)$$

$$\times \int_0^\infty \exp \{-\mu[x/\sin \alpha + x/\sin (2\theta - \alpha)]\}dx, \quad (24)$$

or

$$I_{2\theta} = (K/\mu)[\{\sin (2\theta - \alpha)\}/$$

$$\{\sin \alpha + \sin (2\theta - \alpha)\}]. \quad (25)$$

Relating the intensity at any angle to that at $2\theta = 2\alpha$

$$I_{2\theta}/I_{2\theta=2\alpha} = (1/2)\{[\sin (2\theta - \alpha)]/$$

$$[\sin \alpha + \sin (2\theta - \alpha)]\}. \quad (26)$$

For a cylindrical sample completely bathed in a primary beam, the absorption correction has been determined by means of a graphical integration and the results are plotted elsewhere for convenient use.[18] This correction is generally smaller for large angle diffraction than that for the flat sample, and hence the cylindrical sample is preferable to the flat sample in this respect. On the other hand, this correction has been computed on the assumption that the cylindrical sample is completely bathed in incident radiation

of uniform intensity across the entire section of the beam, and this is seldom true for crystal monochromated x-rays. It has been shown,[19] however, that no marked change of relative intensity in the diffraction pattern of liquid sodium occurred when several diameters of sample were used, from about two to five times the width of the incident beam.

Use of a crystalline material such as mica for the sample holder has an advantage in that the diffraction produced by it is largely concentrated in sharp spots and hence can easily be distinguished from the true liquid pattern, whereas a glass holder gives a pattern closely similar to that of liquids and hence cannot easily be distinguished from the desired pattern. But the choice of construction for a sample holder is not a simple matter, since considerations of strength, chemical properties, and many other features are also important.

3. Incoherent Radiation and Curve Fitting

In determining the function $i(s)$ from experimental data, it is obviously necessary to have I_{eu} and Nf^2 in the same units. This is done by assuming that at large angles where interference effects can no longer be observed in the diffraction pattern, the observed coherently scattered x-rays have the same intensity as that produced by the same number of atoms which scatter x-rays independently of one another with no interference effects. If the atoms scatter x-rays independently, then the curve for the coherent scattering of N atoms will be of the same form as that for a single atom. These curves can be obtained from tables[20] of atomic structure factors. But before the above fitting of curves can be made, a correction must be applied to the observed intensity curve for incoherent radiation. It is shown elsewhere that the intensity of x-rays scattered from an atom is

$$I = I_e[f^2 + R(Z - \sum f_n{}^2)], \quad (27)$$

where I_e is the Thompson scattering per electron, f is the atomic structure factor, f_n is the structure factor of the nth electron in the atom, Z is the atomic number, and R is a recoil factor defined as

$$R = 1/(1 + \{h/mc\lambda\} \text{ vers } \phi)^3.$$

DIFFRACTION OF X-RAYS BY LIQUID ELEMENTSIn the above expression for I, the term $I_e f^2$ is identified with coherent scattering and the term $I_e R(Z - \Sigma f_n^2)$ is identified with incoherent scattering which plays no part in interferences, but which introduces a slowly varying background on all patterns. The incoherent scattering function is conveniently tabulated elsewhere.[21] The following intensity ratios are useful in the curve-fitting process:

Incoherent/Total

$$= [R(Z - \textstyle\sum F_n^2)]/[f^2 + R(Z - \textstyle\sum f_n^2)], \quad (28)$$

$$\text{Incoherent/Coherent} = [R(Z - \textstyle\sum f_n^2)]/f^2, \quad (29)$$

$$\text{Coherent/Total} = f^2/[f^2 + R(Z - \textstyle\sum f_n^2)]. \quad (30)$$

Thus, for example, if the observed intensity has been corrected for polarization and absorption, and if at some large angle of scattering, there is no evidence of interference peaks, then the amount of incoherent radiation at that point can be obtained from Eq. (28). The difference between the total and the incoherent will be the coherent. Knowing the coherent intensity at this point enables one, from the f^2 tables, to draw in the independent coherent scattering at all angles. From this, and Eq. (29), the incoherent scattering at all angles can be drawn in, and subtracted from the observed intensity at all points, thus giving the I_{eu} to be used in the function $i(s)$, along with the coherent or Nf^2 curve. It is perhaps clearer to note that what has been done is to use

$$[(I_{eu}/N)/f^2] - 1 \text{ for } i(s).$$

The incoherent correction for elements of high atomic number is very small but for elements of low atomic number, it is quite large. When the incoherent correction is small, the recoil factor may be taken as unity without introducing appreciable error.

One important requirement of the theory is that the experimental curve be known accurately to very large values of s, where $s = \{4\pi \sin \theta\}/\lambda$. This is important for two reasons, first, because all the interference effects should be included in the analysis, and second, because it is essential that the fitting shall be made at a point where the scattering is as completely independent as

possible. Experimentally, it has not been possible, because of the weakness of the radiation, to carry the experimental observations much beyond $s = 12$, but it is possible that future refinements will be in the nature of improved experimental technique to extend the range of s beyond that which is now practicable. It has been shown that in one particular case,[22] slight extension of this range has not markedly altered the results obtained, although in other cases, extension of the range has had considerable effect on the final result.

Because of the low intensity of coherent radiation at large angles where this curve-fitting is performed, much uncertainty in the whole analysis can be introduced at this step unless special attention is given to careful intensity determination at large angles. One partially successful attempt[23] has been made to minimize reliance upon the exact determination of weak coherent intensity at one value of the angle of diffraction, as is usually done. In effect, it is an attempt to perform the curve-fitting process over the whole curve rather than at one point.

4. The Analysis

After the intensity function $i(s)$ has been determined, the remaining problem is to evaluate the integral in the expression

$$4\pi r^2 \rho(r) = 4\pi r^2 \rho_0 + (2r/\pi) \int_0^\infty si(s) \sin rs\, ds. \quad (31)$$

Three methods have been used for this purpose: (1) the use of an harmonic analyzer, (2) graphical integration, and (3) trigonometric interpolation. A brief description of these three methods will be given.

Consider, first, for example, the use of the Coradi analyzer. If r is taken as a multiple of some chosen constant r_0, then $r = nr_0$ where n is the order of a harmonic and, if the function $si(s)$ is expressed as a sine series,

$$si(s) = \sum_0^\infty A_n \sin nsr_0;$$

then it can be shown[24] that

$$A_n = (1/\pi) \int_0^{2\pi} si(s) \sin nr_0 s\, ds$$

and the Coradi analyzer gives nA_n directly as the reading of the instrument after tracing over the $si(s)$ curve with gears in place for harmonic n. The ordinate scale for the $si(s)$ curve may be chosen for any convenient use with the instrument and the appropriate linear scale factor must then be applied to the reading obtained. Choice of the abscissa scale is determined by the construction of the analyzer and by the constant r_0. It is desired that the range of the argument, sr_0n, shall be equal to the total range of abscissa of the instrument, $2\pi n$, which covers 40 cm in the usual type of Coradi analyzer. Thus the limiting value of s, designated s_0, is related to r_0 by the relation $s_0r_0n=2\pi n$ or $s_0=2\pi/r_0$. If points on the distribution curve are desired at intervals of 0.4A, $r_0=0.4$, or $s_0=15.7$ and hence we have 40/15.7 or 2.55 cm per s unit. Plotting the abscissa as 2.55 s will then supply 0.4A per harmonic. Similarly, by use of 2.80 s we obtain 0.44 per harmonic. Gears could be constructed to supply fractional harmonics, or the existing gears can be interchanged from one range to another to give fractional harmonics. Thus, for example, over certain intervals, this procedure has supplied data for every 0.1A. Integration limits from 0 to 2π are required by the instrument rather than the desired limits of 0 to ∞, but since the function $si(s)$ is zero beyond the point of curve-fitting, as far as experiment is able to show, and since r_0 is chosen to include all the available data in the range of abscissa of the instrument, then this limited range of integration is permissible.

The integral of Eq. (31) can be evaluated by means of graphical integration. If $\beta=nr_0s$ and r_0 is taken as 0.4A, then β (in degrees) $=22.92ns$, and cards can be made listing $\sin \beta$ as a function of s for any n which is desired. Multiplying $si(s)$ and $\sin \beta$, plotting this product as a function of s and planimetering the area under this curve gives the required result for one value of r. In this method, the number of curves to be computed, plotted, and planimetered is the same as the number of points in the distribution curve. A variation of this scheme is to plot $si(s)$ against s (or $\sin \theta/\lambda$ for further simplification), draw the reflection of this curve to obtain an envelope, prepare cards for each harmonic with the abscissae indicated where the sine function takes

on values of 0, 0.5, 0.866, 1.0 over a complete cycle, determine $si(s) \sin nr_0s$ from these cards and the envelope, and finally planimeter as before. In this way, several determinations can be made within one envelope.

The method of trigonometric interpolation has been used by Danielson and Lanczos[25] to evaluate the integral of Eq. (31). This method depends on expressing the $si(s)$ curve in an approximate analytical form, a finite trigonometric series, chosen in such a way that the integral for each of a chosen set of values of r becomes simply related to one of the coefficients of the series. The s axis of the $si(s)$ curve is divided into some number, say 36, equal intervals. Arithmetic manipulation of the ordinates at these points of the $si(s)$ curve, together with a companion list of sine functions, gives the desired result. Prepared forms[25] greatly facilitate this procedure.

IV. RESULTS

1. Helium

Working under exceedingly difficult experimental conditions, Keesom and Taconis[26] passed Cu $K\alpha$ filtered radiation through free streams of liquid He I ($-270.5°C$) and He II ($-271.4°C$). Stream diameters of 1.5 mm and 3.0 mm were used, and in all cases the diffraction patterns had dense backgrounds which presumably were due largely to incoherent radiation. In both He I and He II, the position of the one observed peak was determined to be $\sin \theta/\lambda=0.157$. No complete analysis was attempted, to obtain a distribution curve, but an analogy was made between the observed pattern and that to be expected from smeared-out crystal models, following the method of Prins and Petersen.[27] It was concluded that the liquid structure was more nearly similar to that of a face-centered cubic type than to that of a diamond-like structure.

2. Lithium

This element (m.p. 186°C) was investigated at 200°C by Gamertsfelder.[28] In a cylindrical camera of 9.20-cm radius, the sample had a horizontal cross section in the shape of a right isosceles triangle with the incident, crystal-reflected, Mo $K\alpha$ radiation passing 1.8 cm through the liquid along the altitude of the triangle. Because of the large
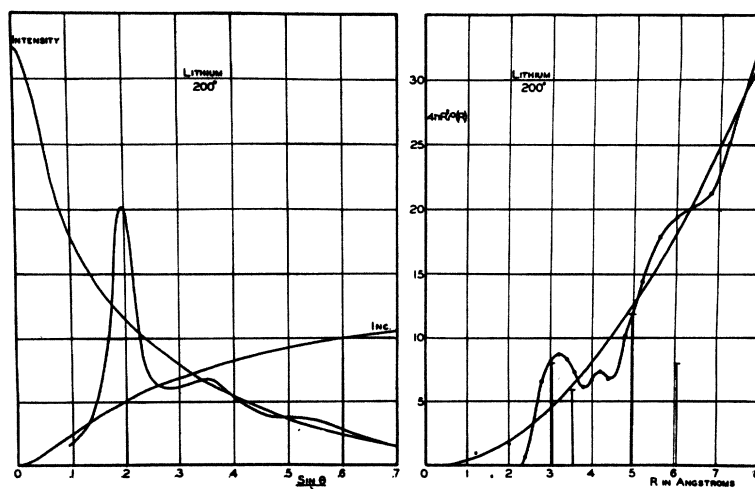
FIG. 5. Intensity curve and distribution curve for liquid lithium at 200°C. Ideal crystalline distribution out to 6A shown by vertical lines.

sample size relative to that of the camera, considerable blurring of the pattern is to be expected, and hence some uncertainty is introduced in the distribution curve on this account. Very thin mica windows were used to minimize undesirable scattering. Figure 5 shows the intensity curve plotted to an arbitrary ordinate scale, and the distribution curve, together with vertical lines to represent the ideal distribution in the crystalline form. The unusually large incoherent correction to the observed intensity is noted on the intensity graph of Fig. 5. The first peak in the distribution curve occurs at about 3.24A and it represents a concentration of roughly 9.8 atoms. The small second peak at 4.2A is not correlated closely with any distance in the crystal.

3. Nitrogen

Liquid nitrogen has been studied by Keesom and de Smedt[7] and by Sharrah[29] and nitrogen gas under high pressures has been studied by Harvey.[30] In the early work of Keesom and de Smedt, peaks in the intensity pattern were reported at sin $\theta/\lambda = 0.139$ and 0.208, but in the recent work of Sharrah, who used monochromatic Mo $K\alpha$ radiation, intensity peaks were found at sin $\theta/\lambda = 0.144$, 0.26, and 0.42 for nitrogen at 89°K, and at 0.148, 0.26, and 0.42 for 64°K. Figure 6 shows the results obtained by Sharrah. The first intensity peak is very prominent, whereas the other peaks are quite weak. Peaks

in the distribution curve are at nearly the same distances for both temperatures: 1.3A, 2.6A, 4.0A, and 4.8A. The areas under the first peaks are 1.03 for 89°K and 1.08 for 64°K, and these peaks are discrete, implying permanent neighbors. Within the precision of this determination, the number of nearest neighbors is one, which confirms the existence of the N_2 molecule in liquid nitrogen. Harvey[30] showed that for compressed nitrogen gas, the x-ray scattering at small angles decreases as the pressure is increased.

4. Oxygen

Keesom and de Smedt[7] observed intensity peaks in the pattern from liquid oxygen, at sin $\theta/\lambda = 0.154$, 0.24, and 0.35. Sharrah and Gingrich[31] more recently have used monochromatic radiation and they report intensity peaks at sin $\theta/\lambda = 0.157$, 0.35, and 0.5 for the 89°K case, and at 0.159, 0.35, and 0.5 for the 62°K case. Their intensity curves are shown in Fig. 7, together with the distribution curves for the two temperatures. Peaks in these latter curves occur at 1.3A, 2.2A, 3.4A, and 4.2A for 89°K, and at 1.25A, 2.15A, 3.2A, and 4.1A for 62°K. The area under the first 89°K peak is 1.08 while that for 62°K is 1.18. Considering experimental precision, it is believed that the 1.08 is not significantly different from unity, and it is somewhat doubtful
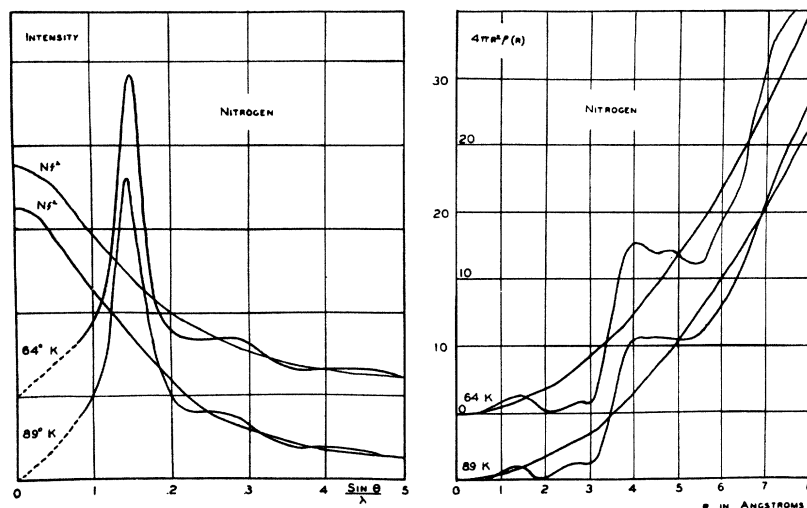
FIG. 6. Intensity curves and distribution curves for liquid nitrogen
at 64°K and 89°K.
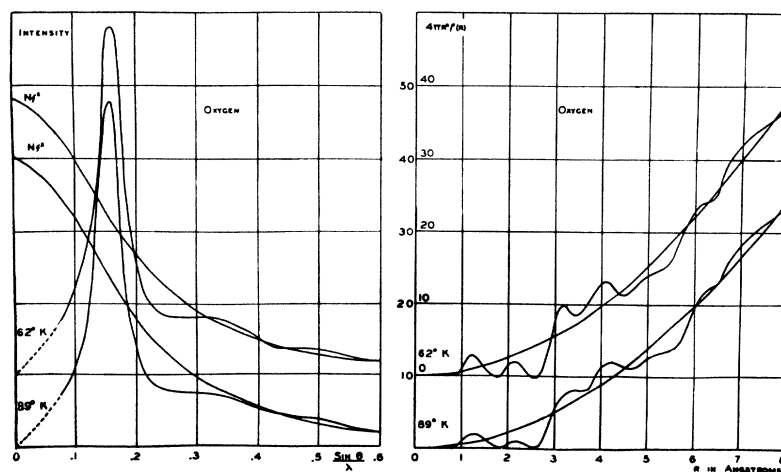
FIG. 7. Intensity curves and distribution curves for liquid oxygen
at 62°K and 89°K.

whether the 1.18 should be interpreted as giving unambiguous proof of the existence of slightly more than one atom, on the average, at this distance. At both temperatures, a second discrete peak persisted in all determinations, a feature which is unique in liquid elements so far studied, to liquid oxygen. The occurrence of this second, discrete peak, and the excess areas under the first peak are suggestive of the presence of O_3 in liquid oxygen, since in this form, some atoms would have two nearest neighbors at about 1.3A, and some other atoms would have one nearest neighbor at 1.3A and one neighbor at 2.2A which is the

approximate distance of the observed second peak. Existence of the third and fourth peaks have not been cited as clear-cut evidence for the presence of larger aggregates of oxygen atoms.

5. Sodium

Work on liquid sodium (m.p. 97.5°C) has been reported by Keesom,[32] Randall and Rooksby,[33] Tarasov and Warren,[34] and Trimble and Gingrich.[35] Quantitative work using monochromatic radiation was attempted in the last two cases, and their results are in essential agreement. Figure 8 shows the intensity curves and the

distribution curves. Intensity peaks occur at $\sin \theta/\lambda = 0.162$, 0.29, and 0.42 for 100°C and at 0.157, 0.28, and 0.4 for 400°C. The first peak in the distribution curve is at about 3.83A for 100°C and at about 3.90A for 400°C. These two distribution curves give an excellent illustration of the smearing-out effect on the distribution curve due to increased thermal agitation of the atoms for the liquid at high temperatures.

Using a simplified model of the liquid state, Wall[36] has calculated with considerable success

the latent heats of fusion and of vaporization for sodium from the distribution curves given here.

6. Aluminum

Randall and Rooksby[37] and Gamertsfelder[28] have reported work on liquid aluminum (m.p. 659°C). In the more recent work,[28] the sample was simply an aluminum wire heated by means of a gas flame, with the very thin oxide coat acting as the sample holder. Figure 9 shows the intensity and the distribution curves for 700°C.
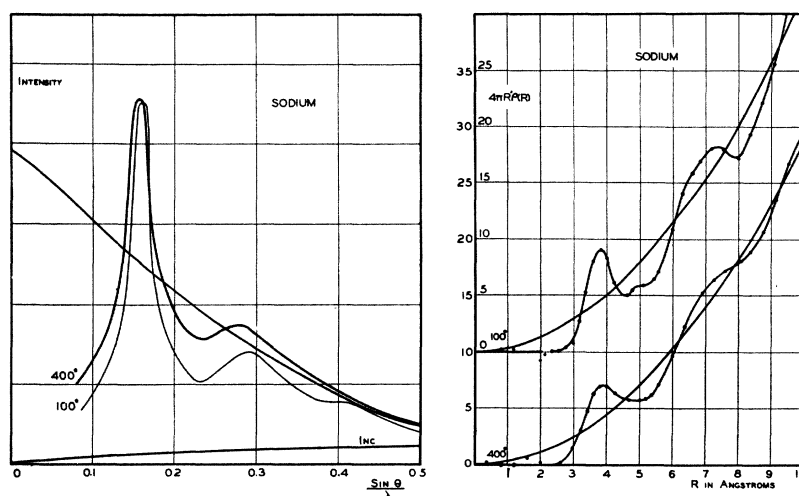
FIG. 8. Intensity curves and distribution curves for liquid sodium
at 100°C and 400°C.
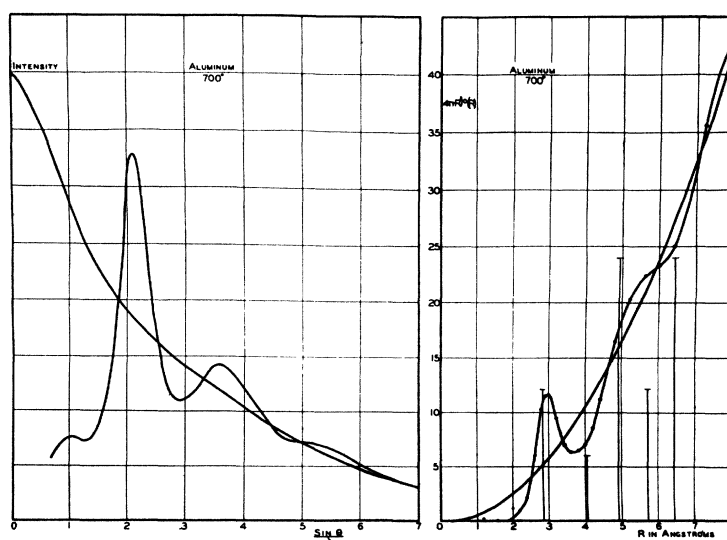
FIG. 9. Intensity curve and distribution curve for liquid aluminum at 700°C.
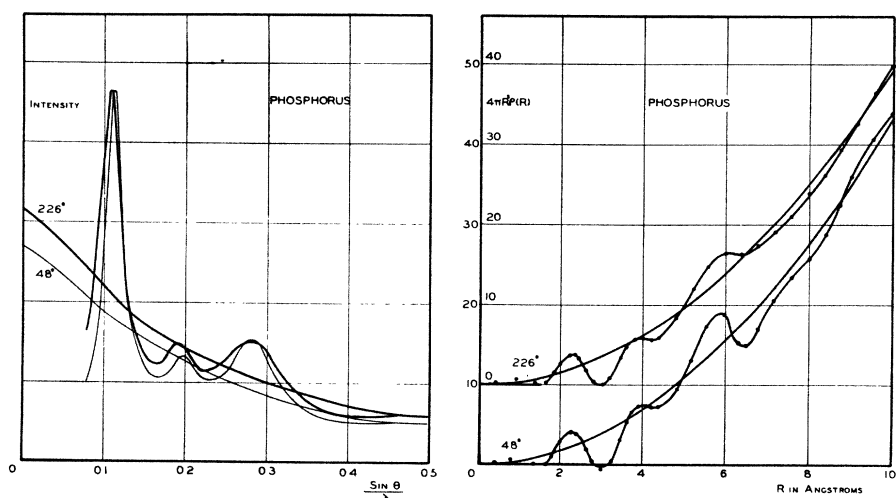
FIG. 10. Intensity curves and distribution curves for liquid yellow
phosphorus at 48°C and 226°C.

In the intensity curve, a very weak peak ap-
peared at $(\sin\theta)/\lambda = 0.10$, and the other peaks,
whose intensities fall off in roughly the usual
manner, occur at 0.210, 0.36, and 0.55. The first
peak in the distribution curve is at 2.96A, it is
not discrete, and the area under it represents
about 10.6 atoms. It is seen that in this case,
there is a fair correlation with the structure of
the crystal. As in other cases where the first
distribution peak is not discrete, the nearest
neighbors are constantly changing, and what one
gets is an average number of nearest neighbors,
with frequent interchanging of these neighbors.

7. Phosphorus

The only work on liquid yellow phosphorus
(m.p. 44.1°C) was reported by Thomas and
Gingrich.[38] Their intensity and distribution
curves for temperatures 48°C and 226°C are
shown in Fig. 10. Intensity peaks occur at
$(\sin\theta)/\lambda = 0.111$, 0.198, 0.28, for 48°C, and at
0.108, 0.194, and 0.28 for 226°C. Peaks in the
distribution curves are found at very nearly the
same distances for both temperatures, 2.25A,
3.9A, and 6.0A. Of particular interest here, is the
fact that the first of these peaks at both tempera-
tures is discrete, and represents approximately
three atoms, thus showing that in liquid yellow
phosphorus, each atom has three permanent
nearest neighbors. This confirms, very directly,

the existence of P_4 molecules in liquid yellow
phosphorus. Rushbrooke and Coulson[39] have
identified the second and third peaks with fre-
quently recurring distances between atoms which
are not in the same P_4 molecule.

Both red and black phosphorus occur in an
amorphous form, and the atomic distribution
curve has been determined in these cases.[23,38]
Here again there are three permanent nearest
neighbors at a distance (2.28A) slightly (perhaps
insignificantly) greater than that in liquid yellow
phosphorus (2.25A). Beyond the first peak, how-
ever, the distribution curves differ considerably.

8. Sulphur

Blatchford,[40] Das,[41] Das and Das Gupta,[42]
Prins,[43] and Gingrich[44] have reported work on
this element (m.p. 113°C or 119°C). Although
interesting information has been supplied in all
cases, a complete analysis has been given in only
one case,[44] for which the intensity and distri-
bution curves are shown in Fig. 11. At tempera-
tures of 124°C, 166°C, 175°C, 225°C, and 340°C,
complete analyses were made, though intensity
patterns were obtained at other temperatures, to
determine more exactly the temperature at which
considerable change in the position of the main
peak occurred. This change was found to take
place between 157°C and 166°C. In the distri-
bution curves at all temperatures, the nearest
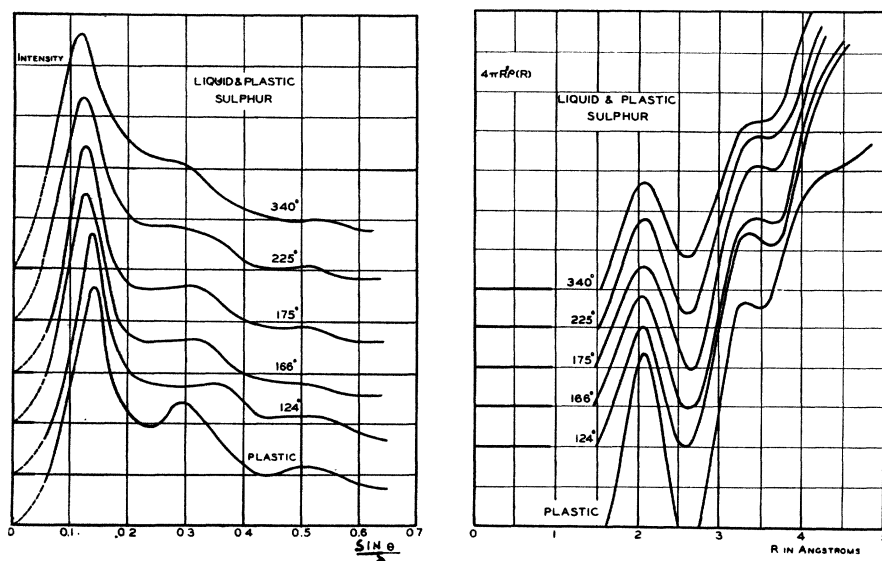
FIG. 11. Intensity curves and distribution curves for liquid sulphur at 124°C, 166°C, 175°C, 225°C, 340°C, and for plastic sulphur at room temperature.
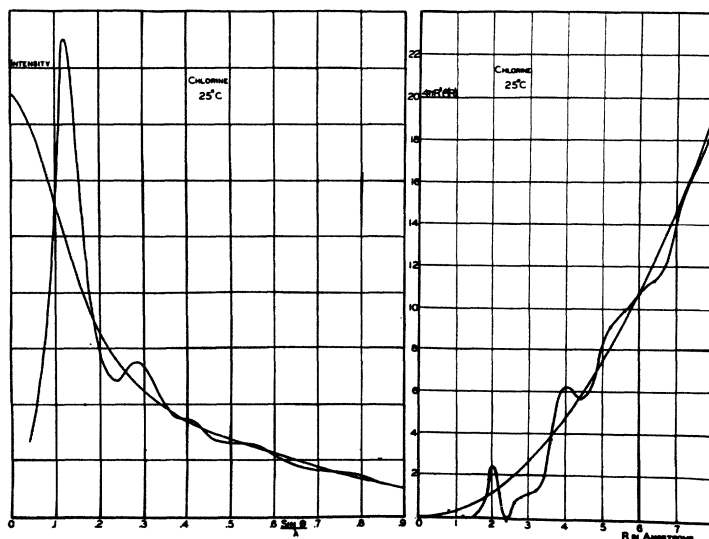
FIG. 12. Intensity curve and distribution curve for liquid chlorine at 25°C and 7.7 atmospheres pressure.

neighbor distance is about 2.07A, and these approximately 1.7 nearest neighbors are indicated as being permanent for temperatures up to about 200°C. It is pointed out that if the S_8 molecule were in the form of an open chain, then the end atoms would have one nearest neighbor, and the intermediate atoms would have two nearest neighbors, giving rise to an average of roughly 1.7 atoms as observed. For plastic sulphur at room temperature, there are two permanent neighbors at 2.08A, characteristic of a closed ring, or of a long chain.

9. Chlorine

Liquid chlorine (b.p. 34.6°C) was investigated by Gamertsfelder[28] at 25°C and under its own vapor pressure of about 7.7 atmospheres. Figure 12 shows the results of this work, with intensity
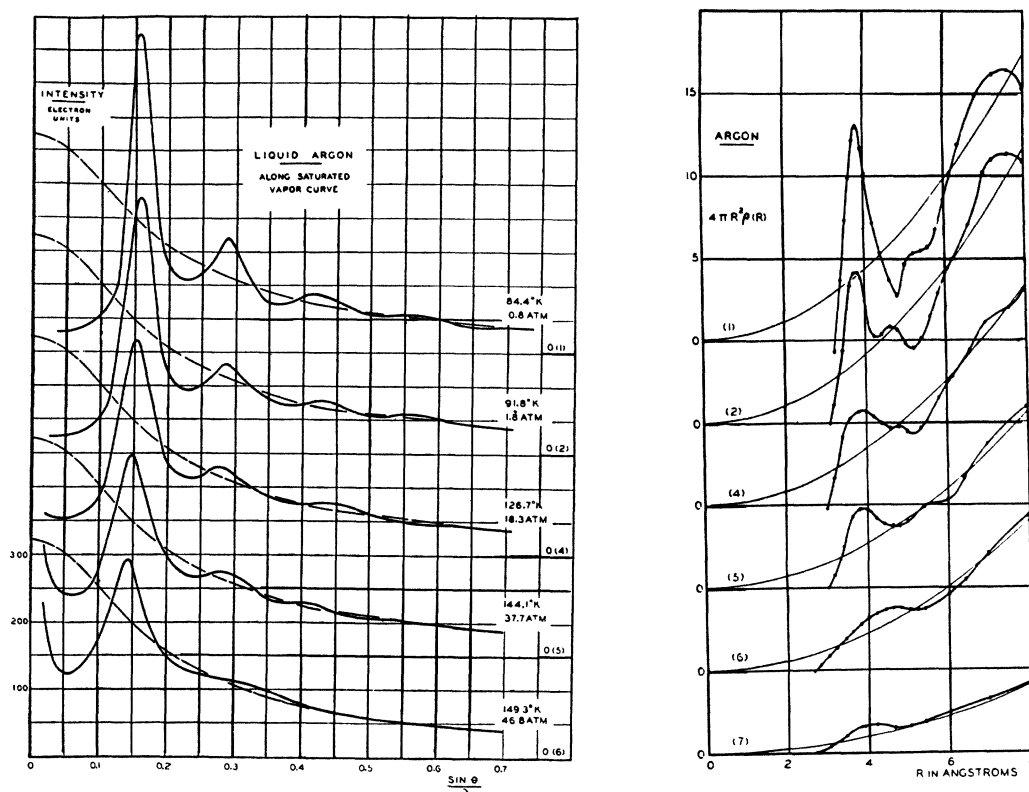
FIG. 13. Intensity curves and distribution curves for liquid argon at 84.4°K and 0.8 atmos.; 91.8°K and 1.8 atmos.; 126.7°K and 18.3 atmos.; 144.1°K and 37.7 atmos.; 149.3°K and 46.8 atmos.; and a distribution curve (No. 7) for argon gas at 149.3°K and 43.8°K.

peaks at (sin θ)/λ = 0.122, 0.285, 0.41, 0.55, and 0.8 and with distribution peaks at 2.01A, 2.0A, and 5.2A. The peak at 2.01A represents one (0.97 measured) permanent nearest neighbor, confirming the existence of Cl_2 molecules in the liquid.

10. Argon

In many respects, this element (m.p. 189.2°C; b.p. 185.7°C) is one of the most interesting and suitable to study. Work has been reported by Keesom and de Smedt,[7] Lark-Horovitz and Miller[45] and Eisenstein and Gingrich.[46,47] In the latest work,[47] diffraction patterns have been obtained for the liquid and for the vapor over wide ranges of pressure and temperature. Intensity and distribution curves are shown in Fig. 13 for a few conditions of pressure and temperature, with argon in the liquid state for curves 1, 2, 4, 5, and 6, and in the vapor state for curve 7 (distribution curve only). Many more curves are shown

in the original article, particularly for argon vapor, and reference should be made to this article for more detailed results. Referring to the intensity curves of Fig. 13, at least three effects can be observed of the increase in temperature along the saturated vapor curve. The most obvious effect is the progressively greater smearing-out of the pattern; another observation is that the position of the main peak is progressively shifted to smaller angle; and a third effect is the increase in the small angle scattering at high temperatures. This last effect is even more pronounced in the case of high temperature, high pressure vapor, and it is interpreted as being due to the formation of many or of frequently recurring large-scale (10A or greater) density fluctuations, under these conditions. The distribution curves show the most pronounced first peak at low temperatures as expected. Whereas in crystalline argon there are 12 nearest neighbors at 3.82A, in liquid argon at 84.4°K and 0.8 atmos.
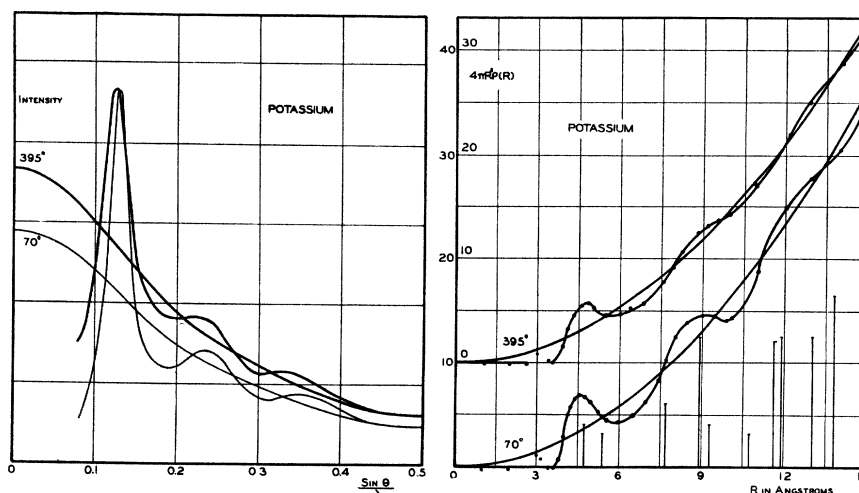
Fig. 14. Intensity curve and distribution curve for liquid potassium.
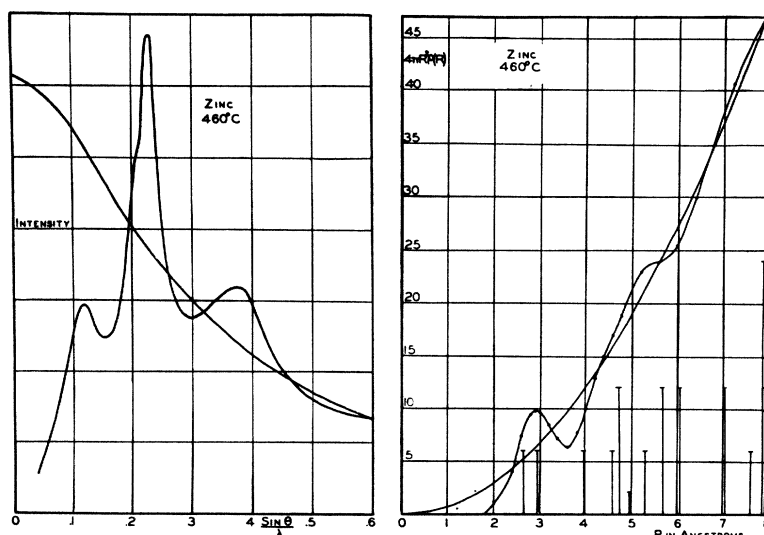
Fig. 15. Intensity curve and distribution curve for liquid zinc at 460°C.

there are 10.2 to 10.9 nearest neighbors at 3.79A. These results show that relatively small changes of temperature have considerable effect on the distribution curve of argon near its triple point.

Theoretical considerations relative to atomic distribution curves have frequently made reference to liquid argon. Details of the several approaches to this problem and of the results so far obtained may be found in the work, for example, of Wall,[36] Rice,[48] Rushbrooke and Coulson,[39] Rushbrooke,[49] Corner and Lennard-Jones,[50] Kirkwood,[51] and Kirkwood and Boggs.[52]

11. Potassium

Liquid potassium (m.p. 6ℓ.3°C) has been studied by Keesom[32] and by Randall and Rooksby[33] at one temperature just above the melting point, and by Thomas and Gingrich[53] at the two temperatures 70°C and 395°C. Curves from this latter work are shown in Fig. 14. At 70°C intensity peaks occur at $(\sin \theta)/\lambda = 0.130$, 0.233, 0.36, whereas at 395°C peaks were found at 0.126, 0.22, and 0.35. In the distribution curves, the first peak is at 4.64A for 70°C and at 4.76A for 395°C, with both peaks representing an average concentration
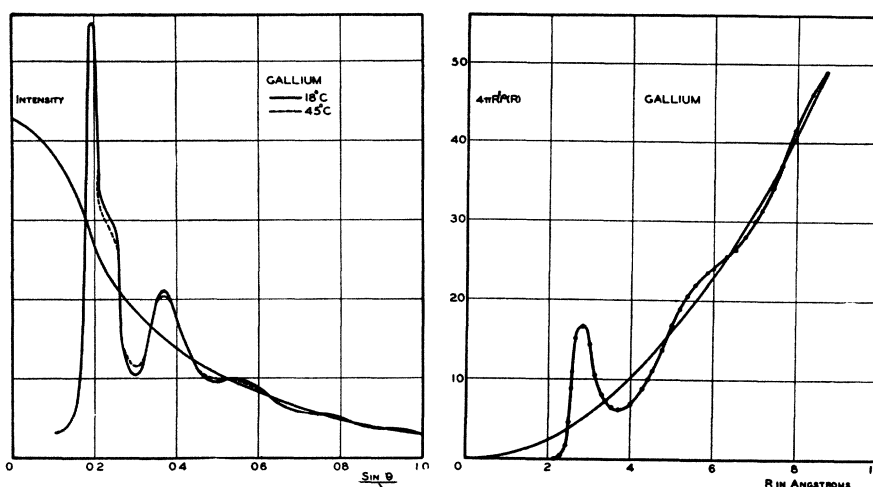
Fig. 16. Intensity curves for liquid gallium at 18°C and 45°C and a distribution
curve for liquid gallium at 18°C.

of about 8 atoms. These results have been used by
de Boer and Michels,[54] Hildebrand,[55] and Gingrich
and Wall[56] in their theoretical discussions relative
to atomic distributions. In the latter case, for
example, the latent heats of fusion and of
vaporization of potassium have been calculated
with some success, using the distribution curves
shown here. Hildebrand has also calculated from
these distribution curves the ratio of the energy
of vaporization at these two temperatures, ob-
taining surprisingly close agreement with that
from the vapor pressure curve.

12. Zinc

The only investigation on liquid zinc (m.p.
419°C) has been made by Gamertsfelder[28] at
460°C. Figure 15 shows the intensity and distri-
bution curves in this case. As in the case of
aluminum, the first intensity peak is weak, and
the second peak is the most intense. The intensity
peaks occur at $(\sin \theta)/\lambda = 0.115$, 0.228, 0.38. The
first distribution peak at 2.94A represents an
average concentration of about 10.8 atoms.

13. Gallium

Liquid gallium (m.p. about 30°C, and easily
undercooled) has been studied by Menke[57] at 18°
and at 45°C. Results of this work are shown in
Fig. 16. Intensity peaks occur at $(\sin \theta)/\lambda = 0.195$,
0.372, 0.57, 0.77, and 0.96, and distribution peaks

occur at 2.83A and 5.8A. It is to be noted that
there is but slight difference between the intensity
patterns at the two temperatures in spite of the
fact that at 18°C, the liquid is undercooled.

14. Selenium

The only reported work on liquid selenium
(m.p. 217°C) is that of Prins[43] who simply lists
"spacings" equivalent to intensity peaks at
$(\sin \theta)/\lambda = 0.148$, 0.280, 0.435, states that there
was no appreciable effect of temperature on the
pattern, and notes that the pattern was indentical
with one obtained from a preparation quenched
by dropping into water. Lark-Horovitz and
Miller[58] have worked with amorphous selenium,
obtaining intensity peaks at $(\sin \theta)/\lambda = 0.146$,
0.289, 0.443 and distribution peaks at 2.35A,
3.7A, and 4.8A.

15. Rubidium

Liquid rubidium (m.p. 38.4°C) has been re-
ported by Randall and Rooksby[33] as giving a
diffraction pattern with an intensity peak at
$(\sin \theta)/\lambda = 0.122$

16. Cadmium

Gamertsfelder[28] has worked with liquid cad-
mium (m.p. 321°C) at 350°C. His results are
shown in Fig. 17. Intensity peaks occur at
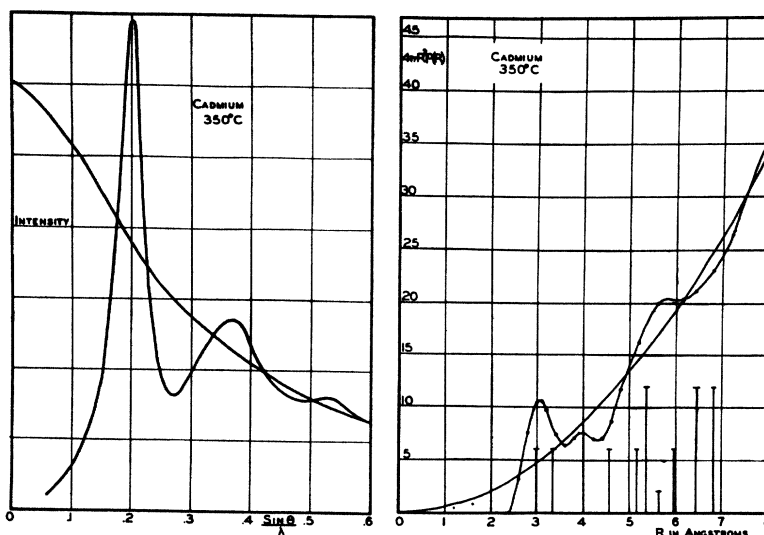
FIG. 17. Intensity curve and distribution curve for liquid cadmium at 350°C.
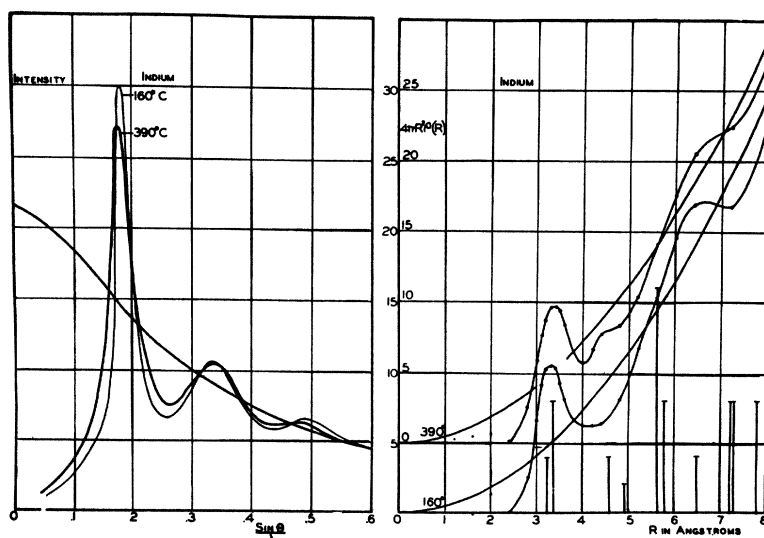
FIG. 18. Intensity curves and distribution curves for liquid
indium at 160°C and 390°C.

$(\sin \theta)/\lambda = 0.203$, 0.360, 0.55 and the first distribution peak, representing an average concentration of 8.3 atoms, is at 3.06A.

17. Indium

Liquid indium (m.p. 155°C) has been studied by Gamertsfelder[28] at 160°C and at 390°C. The results of his work are shown in Fig. 18. The intensity peaks for 160°C are at $(\sin \theta)/\lambda = 0.179$, 0.335, 0.50 and at 390°C they occur at 0.177,

0.335, 0.49. The first distribution peak at 160°C represents about 8.5 atoms at an average distance 3.30A, while that at 390°C represents about 8.4 atoms at roughly 3.36A.

18. Tin

Liquid tin (m.p. 231.9°C) has been dealt with by Sauerwald and Teske,[59] Prins,[43] Danilov and Radtschenko,[60] and Gamertsfelder.[28] In the latter case, temperatures of 250°C and 390°C
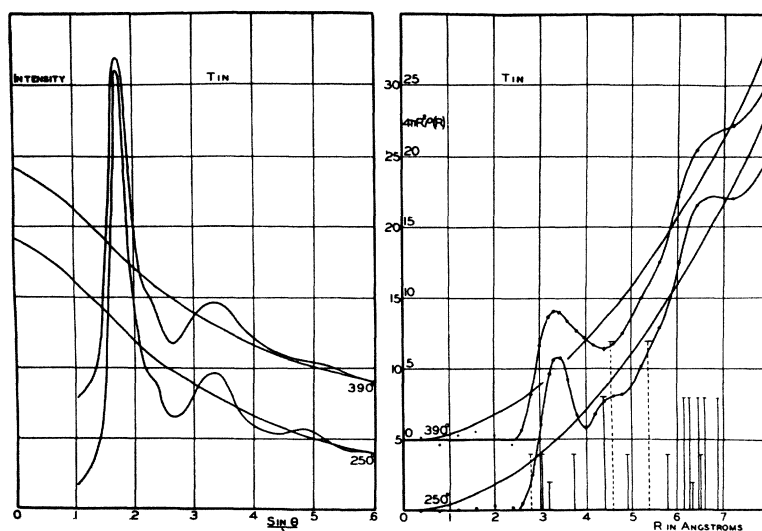
FIG. 19. Intensity curves and distribution curves for liquid
tin at 250°C and 390°C.

were used and these results are shown in Fig. 19. At 250°C, intensity peaks occur at $(\sin\theta)/\lambda = 0.174, 0.335, 0.49$ whereas at 390°C they occur at 0.175, 0.330, 0.50. The first distribution peak for tin at 250°C represents about 10 atoms at 3.38A, and at 390°C, about 8.9 atoms at 3.36A. It is interesting to note from this work that the liquid structure is much more analogous to that of crystalline white tin than to that of crystalline gray tin.

19. Cesium

Randall and Rooksby[33] report having found an intensity peak in the diffraction pattern of liquid cesium (m.p. 28.5°C) at $(\sin\theta)/\lambda = 0.111$.

20. Mercury

Liquid mercury (m.p. 38.9°C) has been investigated by Prins,[61] Coster and Prins,[62] Wolf,[63] Raman and Sogani,[64] Debye and Menke,[9, 65] Sauerwald and Teske,[59] Menke,[57] and Boyd and Wakeham.[66] Most of these investigations led to interesting qualitative results, but the investigations of Debye and Menke,[9, 65] Menke,[57] and Boyd and Wakeham[66] have supplied more detailed information. The results of Debye and Menke[9] are shown in Fig. 20 for mercury at room temperature. Intensity peaks occur at $(\sin\theta)/\lambda = 0.162, 0.328, 0.52, 0.68, 0.82$, and distribution

peaks occur at 3.23A and 6.5A. Using the reflection method, as did Debye and Menke, Boyd and Wakeham[66] reported work for temperatures of $-36°C$, $-34°C$, 0°C, 30°C, 75°C, 125°C, 175°C, and 250°C, and, among other differences from previous work, they found an extra intensity peak at small angle. Unfortunately, however, lack of purity of their radiation raises some doubt as to the origin of this peak.[15] Nevertheless, the possible existence of this extra peak should have a relatively small effect on the distribution curve, and their work does supply information for the first time concerning the temperature effect upon the distribution curve for mercury. Hildebrand, Wakeham, and Boyd[67] have used these results to calculate the intermolecular potential in the case of mercury.

21. Thallium

Sauerwald and Teske[59] report the existence of intensity peaks in the diffraction pattern of liquid thallium (m.p. 303.5°C) at $(\sin\theta)/\lambda = 0.164, 0.323, 0.442$.

22. Lead

Randall and Rooksby[68] report an intensity peak for liquid lead (m.p. 327.5°C) at $(\sin\theta)/\lambda = 0.173$.
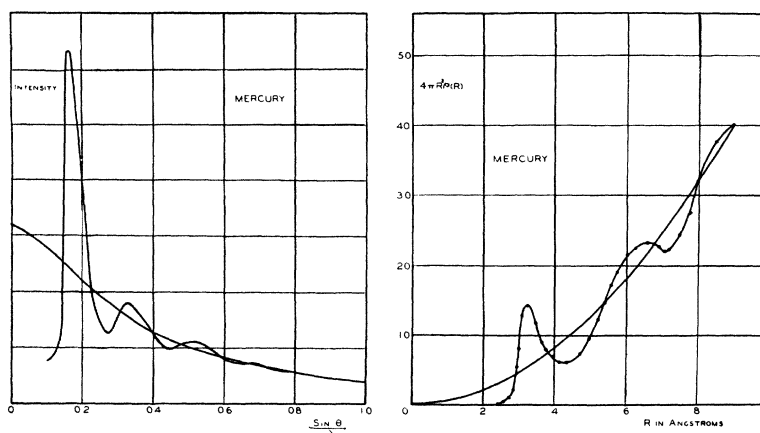
FIG. 20. Intensity curve and distribution curve for liquid
mercury at room temperature.

23. Bismuth

Randall and Rooksby,[68] Sauerwald and Teske[59] and Danilov and Radtschenko[60] report the position of the main intensity peak for liquid bismuth (m.p. 271°C). The average of these three somewhat divergent values is $(\sin \theta)/\lambda = 0.164$.

V. SUMMARY

Experimental work on the diffraction of x-rays by liquid elements has been reported for 23 elements. These determinations in and by themselves are valuable for their contribution to the totality of our knowledge of this particular physical phenomenon. The list of elements for which this information is known should be extended to cover all elements, and it is to be hoped that more complete determinations of the individual diffraction patterns can be given as advances are made in experimental techniques. But a more valuable contribution of this type of work is in making available directly determined descriptions of the structure of various liquid elements, which structure can be correlated with, or used to predict physical properties of the elements.

The structures of liquid elements in terms of the atomic distribution curves have been reported for 16 elements, ten of which reports include determinations of the effect of temperature, and one of which includes the effect of pressure as well. These atomic distribution curves

represent the time-averaged atomic environment about any given atom within the liquid, but this environment is neither permanent, as in a crystal, nor random, as in a gas, and hence no simpler description of liquid structures can now be given to supply the same information. These first 16 determinations of atomic distribution curves constitute the beginning of a complete list of all elements, to parallel a list of the crystal structures of the elements, as an aid to more comprehensive understanding of the structure of matter and of the transitions of matter from one state to another.

Reference has been made, in the present review, to some of the initial attempts toward securing more comprehensive understanding of the structure of matter with the aid of work here reported. On the basis of assumed models of the liquid state, distribution curves have been computed and compared with the observed curves. From these observed distribution curves, interatomic potentials have been deduced, and physical properties of the elements, such as latent heats of fusion and vaporization have been calculated, with some success. In addition to this, the distribution curves have supplied very direct evidence to confirm the existence of molecules in some liquid elements (e.g., N_2, O_2, Cl_2, P_4) and to imply the possible existence of more complicated atomic aggregates in a few cases.

REFERENCES

(1) W. Friedrich, P. Knipping, and M. v. Laue, Sitzb. Math.-Phys. Klasse Bayer. Akad. Wiss. Munchen 303 (1912).

(2) See P. P. Ewald, *Kristalle und Rontgenstrahlen.* (J. Springer, Berlin, 1923); *Handbuch der Physik* (1933), second edition, Vol. 23; R. W. G. Wyckoff, *The Structure of Crystals* (Chemical Catalog Company, New York, 1931).

(3) C. G. Barkla and T. Ayers, Phil. Mag. **21**, 275 (1911).

(4) E. O. Wollan, Rev. Mod. Phys. **4**, 205 (1932).

(5) W. Friedrich, Physik. Zeits. **14**, 397 (1913).

(6) P. Debye and P. Scherrer, Gottingen Nachrichten 16 (1916).

(7) W. H. Keesom and J. de Smedt, Proc. Amst. Akad. Sci. **25**, 118 (1922); **26**, 112 (1923).

(8) F. Zernicke and J. Prins, Zeits. f. Physik **41**, 184 (1927).

(9) P. Debye and H. Menke, Ergeb. d. Tech. Rontgenk. II (1931).

(10) See J. T. Randall, *The Diffraction of X-Rays and Electrons by Amorphous Solids, Liquids and Gases* (John Wiley and Sons, Inc., New York, 1934), p. 107.

(11) P. Debye, Ann. d. Physik **46**, 809 (1915).

(12) B. E. Warren and N. S. Gingrich, Phys. Rev. **46**, 368 (1934).

(13) B. E. Warren, J. App. Phys. **8**, 645 (1937).

(14) A. H. Compton and S. K. Allison, *X-Rays in Theory and Experiment* (D. Van Nostrand Company, New York, 1935), p. 116.

(15) R. Q. Gregg and N. S. Gingrich, Rev. Sci. Inst. **11**, 305 (1940).

(16) C. Gamertsfelder and N. S. Gingrich, Rev. Sci. Inst. **9**, 154 (1938).

(17) A. Eisenstein and N. S. Gingrich, Rev. Sci. Inst. **12**, 582 (1941).

(18) F. C. Blake, Rev. Mod. Phys. **5**, 180 (1933).

(19) G. P. Mitchell, unpublished work done at the University of Missouri.

(20) See reference 14, p. 781.

(21) See reference 14, p. 782.

(22) N. S. Gingrich, Phys. Rev. **59**, 290 (1941).

(23) R. Hultgren, N. S. Gingrich, and B. E. Warren, J. Chem. Phys. **3**, 351 (1935).

(24) See J. W. Mellor, *Higher Mathematics for Students of Chemistry and Physics* (Longmans, Green and Company, 1929), p. 469.

(25) G. C. Danielson and C. Lanczos, J. Frank. Inst. **233**, 365 (1942); **233**, 435 (1942).

(26) W. H. Keesom and K. W. Taconis, Physica **4**, 28 (1937); **4**, 256 (1937); **5**, 270 (1938); Proc. Amst. Akad. Sci. **41**, 194 (1938).

(27) J. Prins and H. Petersen, Physica **3**, 147 (1936).

(28) C. Gamertsfelder, J. Chem. Phys. **9**, 450 (1941).

(29) P. C. Sharrah, Ph.D. Dissertation, University of Missouri, Columbia, Missouri (August, 1942).

(30) G. G. Harvey, Phys. Rev. **46**, 441 (1934).

(31) P. C. Sharrah and N. S. Gingrich, J. Chem. Phys. **10**, 504 (1942).

(32) W. H. Keesom, Proc. Amst. Akad. Sci. **30**, 341 (1927).

(33) J. T. Randall and H. P. Rooksby, Nature **130**, 473 (1932).

(34) L. P. Tarasov and B. E. Warren, J. Chem. Phys. **4**, 236 (1936).

(35) F. H. Trimble and N. S. Gingrich, Phys. Rev. **53**, 278 (1938).

(36) C. N. Wall, Phys. Rev. **54**, 1062 (1938).

(37) Reference 10, p. 134.

(38) C. D. Thomas and N. S. Gingrich, J. Chem. Phys. **6**, 659 (1938).

(39) G. S. Rushbrooke and C. A. Coulson, Phys. Rev. **56**, 1216 (1939).

(40) A. H. Blatchford, Proc. Phys. Soc. London **45**, 493 (1933).

(41) S. R. Das, Ind. J. Phys. **12**, 163 (1938).

(42) S. R. Das and K. Das Gupta, Nature **143**, 332 (1939).

(43) J. A. Prins, Trans. Faraday Soc. **33**, 110 (1937).

(44) N. S. Gingrich, J. Chem. Phys. **8**, 29 (1940).

(45) K. Lark-Horovitz and E. P. Miller, Nature **146**, 459 (1940).

(46) A. Eisenstein and N. S. Gingrich, Phys. Rev. **58**, 307 (1940).

(47) A. Eisenstein and N. S. Gingrich, Phys. Rev. **62**, 261 (1942).

(48) O. K. Rice, J. Chem. Phys. **7**, 883 (1939).

(49) G. S. Rushbrooke, Proc. Roy. Soc. Edinburgh **60**, 182 (1940).

(50) J. Corner and J. E. Lennard-Jones, Proc. Roy. Soc. London **A178**, 401 (1941).

(51) J. G. Kirkwood, J. Chem. Phys. **7**, 919 (1939).

(52) J. G. Kirkwood and E. M. Boggs, J. Chem. Phys. **10**, 394 (1942).

(53) C. D. Thomas and N. S. Gingrich, J. Chem. Phys. **6**, 411 (1938).

(54) J. de Boer and A. Michels, Physica **6**, 97 (1939).

(55) J. H. Hildebrand, J. Chem. Phys. **7**, 1 (1939).

(56) N. S. Gingrich and C. N. Wall, Phys. Rev. **56**, 336 (1939).

(57) H. Menke, Physik. Zeits. **33**, 593 (1932).

(58) K. Lark-Horovitz and E. P. Miller, Phys. Rev. **51**, 380 (1937).

(59) F. Sauerwald and W. Teske, Zeits. f. anorg. allgem. Chemie **210**, 247 (1933).

(60) J. V. Danilov and V. J. Radtschenko, Physik. Zeits. Sowjetunion **12**, 745 (1938).

(61) J. A. Prins, Physica **6**, 315 (1926).

(62) D. Coster and J. A. Prins, J. de phys. et rad. **9**, 153 (1928).

(63) M. Wolf, Zeits. f. Physik **53**, 72 (1929).

(64) C. V. Raman and C. M. Sogani, Nature **120**, 514 (1927).

(65) P. Debye and H. Menke, Physik. Zeits. **31**, 797 (1930).

(66) R. N. Boyd and H. R. Wakeham, J. Chem. Phys. **7**, 958 (1939).

(67) J. H. Hildebrand, H. R. Wakeham, and R. N. Boyd, J. Chem. Phys. **7**, 1094 (1939).

(68) J. T. Randall and H. P. Rooksby, Trans. Faraday Soc. **33**, 109 (1937).